Laser irradiation induced two-photon photolysis of sulfate for photoluminescent sulfur quantum dots

Shuxian Wei[a,b&], Hao Huang[c,d&], Ningning He[a,b], Taiping Hu[a,b], Jijun Huang[e], Yunyu Cai[b], Yixing Ye[b], Pengfei Li[b], Xueling Lei[e*], Changhao Liang[a,b*]*

[a]Department of Materials Science and Engineering, University of Science and Technology of China, Hefei 230026, China

[b]Key Laboratory of Materials Physics and Anhui Key Laboratory of Nanomaterials and Nanotechnology, Institute of Solid State Physics, Hefei Institutes of Physical Science, Chinese Academy of Sciences, Hefei 230031, China

[c]School of Optical Information and Energy Engineering, Wuhan Institute of Technology, Wuhan 430205, China

[d]Department of Materials Science and Engineering, University of Virginia, Charlottesville 22904-4745, USA

[e]Department of Physics, Jiangxi Normal University, Nanchang, Jiangxi 330022, China

*E-mail: pfli@issp.ac.cn (P.F. Li); xueling@mail.ustc.edu.cn (X.L. Lei); chliang@issp.ac.cn (C.H. Liang)

&These authors contributed equally to this work.

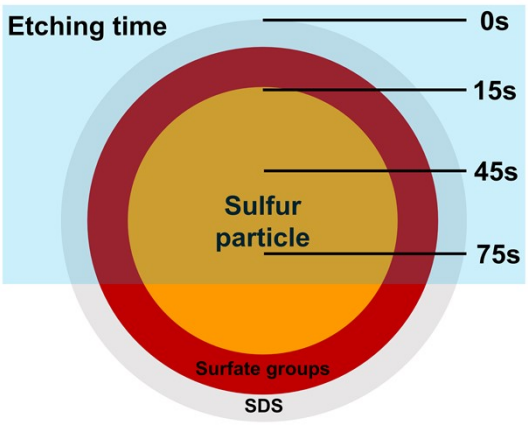

Figure S1. Schematic diagram of structure of SQDs from SDS and the etching process in the XPS.

The sulfur quantum dots (SQDs) is comprised of sulfur particle, sulfate groups on the subsurface, and SDS (Sodium Dodecyl Sulfate) coating on the surface. The sample undergoes ion beam etching at the same location. With prolonged etching time, the etching depth increases correspondingly, facilitating the exploration of additional information within.

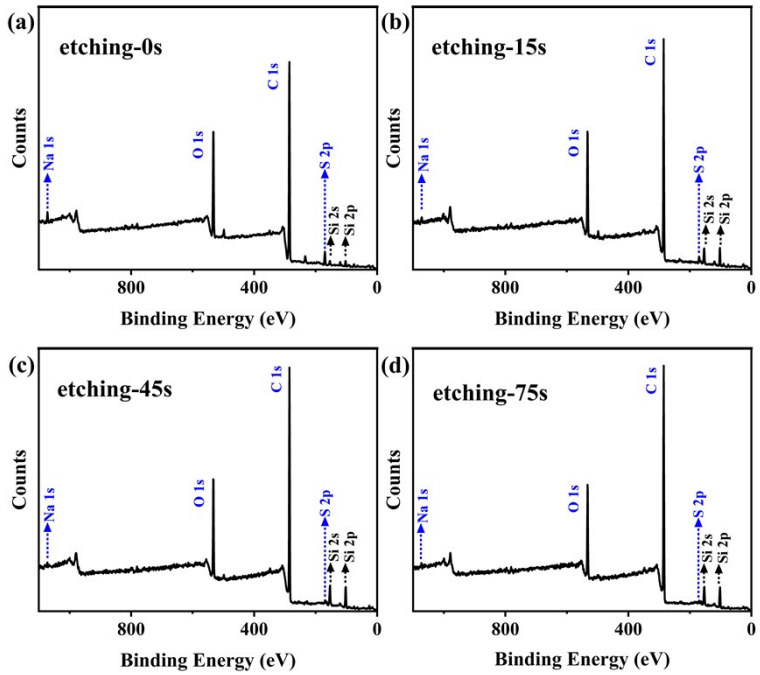

Figure S2. The full XPS spectra of SQDs from SDS with different etching time.

The full XPS spectrum identified Na, O, C, S, and Si elements. The presence of Si may be attributed to impurities from the quartz bottle during laser irradiation or the quartz plate during XPS etching. As the etching depth increased, the Na elements decreased significantly. This corresponds to the structural characteristics of SDS coating. The surface material reduced significantly after etching, leading to the highest signal of Na element in the figure S2(a).

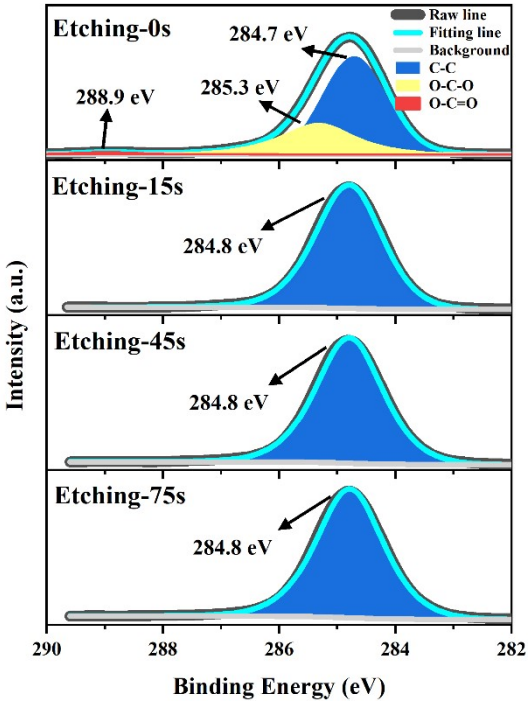

Figure S3. (a) High-resolution C_{1s} XPS spectrum with different ion beam etching time of SQDs.

From C_{1s} XPS spectrum of the sample before etching, three peaks are clearly shown, which is identified to be the C-C peak at 284.7 eV, the O-C-O peak at 285.3 eV, and a weak O-C=O peak at 288.9 eV, respectively. After ion etching to remove surface contamination, only a C-C peak at 284.8 eV is detected, which may originate from the SDS coating on the SQDs.

Thus, we can conclude that these three peaks on the sample surface may originate from contaminated carbon.

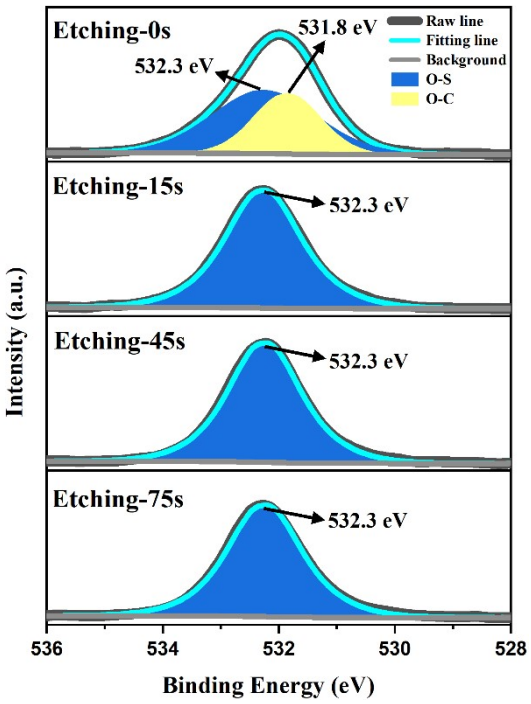

Figure S3. (b) High-resolution O_{1s} XPS spectrum with different ion beam etching time of SQDs.

Table S1. O_{1s} Peak Area at 532.3 eV for 15-75s Etching Times.

Etching Time	Binding Energy (eV)	O_{1s} Peak Area (counts·eV)
15s	**532.3**	**43525.0**
45s	**532.3**	**41983.7**
75s	**532.3**	**39991.2**

Figure S3. (b) shows the high-resolution XPS O_{1s} spectra at different etching times: 0 s, 15 s, 45 s, and 75 s. In each spectrum, the main characteristic peak appears at 532.3 eV, attributed to O-S bonds (blue area). In the 0 s etching spectrum, a peak is also observed at 531.8 eV, corresponding to O-C bonds (yellow area).

Initially, at 0 s of etching, two prominent peaks are observed: 531.8 eV and 532.3 eV. The peak at 531.8 eV corresponds to O-C bonds, indicating the presence of carbon oxides on the sample surface. The peak at 532.3 eV corresponds to O-S bonds, indicating the presence of

oxygen bonded to sulfur in the sample. After 15 s of etching, the peak at 531.8 eV (O-C bonds) is no longer prominent, suggesting the removal of the surface-adsorbed carbon oxide layer. Only the sulfur oxide peak remains. From Table S1, it is evident that as the etching time increases from 15 s to 75 s, the area of the O-S peak at 532.3 eV gradually decreases. This indicates a reduction in sulfur oxides within the sample with increasing etching time.

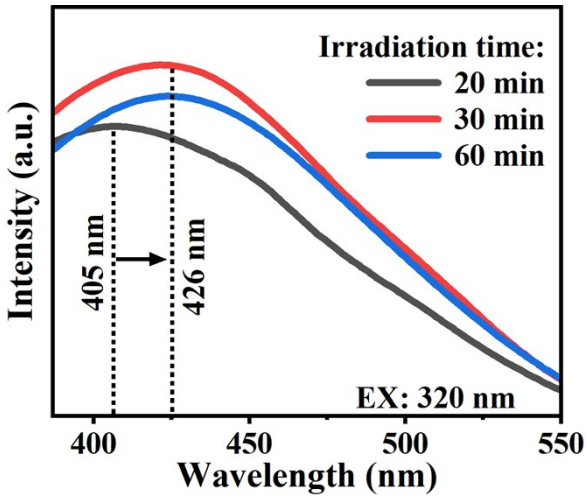

Figure S4. PL spectrum of SQDs from SDS with different irradiation time excited at 320nm.

To explore the growth process of SQDs during the irradiation, the PL of samples with different irradiation time (20-60 min) under excitation wavelength of 320 nm are characterized, as shown in Figure S4. The PL peak has a little red shift and the PL intensity has also been enhanced from 20 to 30 min. In this time range (20-30 min), more and more sulfur elements are generated as the irradiation time extend, thus resulting in the increase in size and quantity of SQDs. As the irradiation time further increase (>30 min), the PL peak will keep unchanged, which means the stability of the size and the saturation of SQDs. However, a significant decrease of the PL intensity can be found, which may be due to the excessive irradiation on the SQDs.

QY (quantum yields) was measured by comparing the integrated photoluminescence intensities and the absorbency values with the reference quinine sulfate (QS). The quinine sulfate (quantum yield = 0.54) was dissolved in 0.1 M H_2SO_4 and the sulfur quantum dots was dissolved in distilled water.[1] To reduce the error, absorbance intensity of the sample in 1.0 cm quartz cell were maintained under 0.05 at the excitation wavelength. Slit widths were set at 10.0 nm when recording their PL spectra. The QE was calculated according to equation (1):

$$Q = Q_R \frac{I A_R \eta^2}{I_R A \eta_R^2} \quad (1)$$

Table S2. PLQY of SQDs.

Sample	Integrated emission Intensity (I)	Abs@ 320 nm (A)	Refractive index of solvent (η)	Quantum Yield@ 320 nm (QY)
Quinine sulfate	192125	0.054	1.33	0.546
Sulphur quantum dots	760	0.023	1.33	0.00519

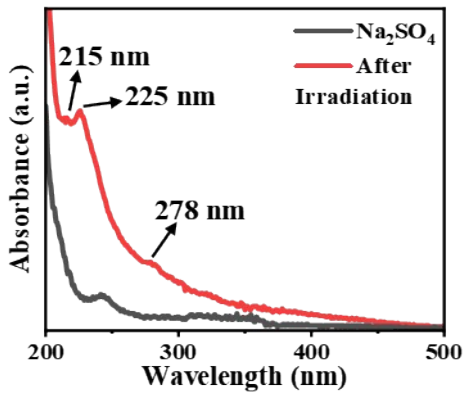

Figure S5. UV absorption spectrum of before and after irradiation 0.1M Na_2SO_4 solution.

Figure S5 depicts the ultraviolet (UV) absorption spectrum of 0.1 M Na_2SO_4 solution before and after irradiation. The intrinsic S-O peak of the Na_2SO_4 solution is observed at 240 nm. After irradiation with a 532 nm laser, new peaks are identified at 215, 225, and 278 nm. Similar to the SQDs from SDS, the absorption peaks at 215 nm and 225 nm are primarily due to the n→σ* transition of numerous heteroatoms (S, O) on the surface.[2–4] Additionally, the absorption peak at 278 nm confirms the formation of sulfur particles, consistent with the experimental results reported in previous studies.[3,5–9]

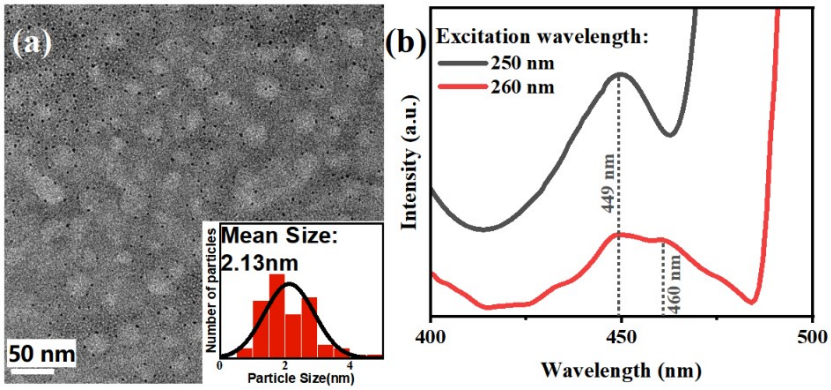

Figure S6. (a) TEM image of SQDs from H_2SO_4, (b) The fluorescence spectrum of SQDs from H_2SO_4 excited at 250-260 nm.

Figure S6(a) displays controlled shape and high dispersity of SQDs from H_2SO_4, with a particle size range of 0.7-4.7 nm and a mean size of 2.13 nm. The small holes in the background of copper mesh are caused by the residual sulfuric acid action in the solution, which also proves stability of the SQDs. Thus, the SQDs show stability in acidic conditions. As shown in Figure S6(b), the SQDs from H_2SO_4 emit fluorescence under an excitation wavelength of 250-260 nm, exhibiting a blue shift in comparison to SQDs coated with SDS. The PL peaks are located around 449nm and 460nm, which indicates a red shift compared to SQDs coated with SDS.

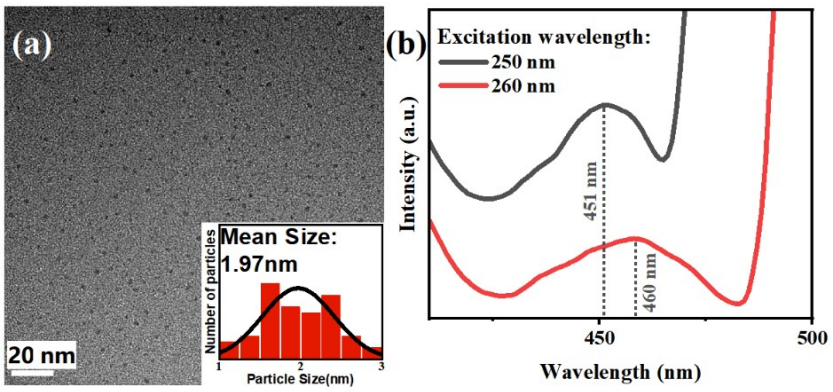

Figure S7. (a) TEM image of SQDs from Na_2SO_4, (b) The fluorescence spectrum of SQDs from Na_2SO_4 excited at 250-260 nm.

As shown in Figure S7(a), the SQDs from Na_2SO_4 have controlled shape and high dispersity, with a particle size in the range of 1-3 nm and a mean size 1.97 nm. Similar with the SQDs from H_2SO_4, the SQDs from Na_2SO_4 exhibit fluorescence under 250-260 nm excitation wavelength (Figure S7(b) and display PL peaks at around 451nm and 460nm.

Reference:

1 D. F. Eaton, *Pure and Applied Chemistry*, 1988, **60**, 1107–1114.
2 L. Shen, H. Wang, S. Liu, Z. Bai, S. Zhang, X. Zhang and C. Zhang, *J. Am. Chem. Soc.*, 2018, **140**, 7878–7884.
3 X. Xie, L. Li, P. Zheng, W. Zheng, Y. Bai, T. Cheng and J. Liu, *Materials Research Bulletin*, 2012, **47**, 3665–3669.
4 G. Qiao, L. Liu, X. Hao, J. Zheng, W. Liu, J. Gao, C. C. Zhang and Q. Wang, *Chemical Engineering Journal*, 2020, **382**, 122907.
5 P. Paralikar and M. Rai, *IET Nanobiotechnology*, 2018, **12**, 25–31.
6 Z. Huang, Y. Gao, Z. Huang, D. Chen, J. Sun and L. Zhou, *Microchemical Journal*, 2021, **170**, 106656.
7 S. Saedi, M. Shokri and J.-W. Rhim, *Arabian Journal of Chemistry*, 2020, **13**, 6580–6588.
8 J. Häcker, D. H. Nguyen, T. Rommel, Z. Zhao-Karger, N. Wagner and K. A. Friedrich, *ACS Energy Lett.*, 2022, **7**, 1–9.
9 S. Shankar, R. Pangeni, J. W. Park and J.-W. Rhim, *Materials Science and Engineering: C*, 2018, **92**, 508–517.